

# Everything Perturbed All at Once: Enabling Differentiable Graph Attacks

Haoran Liu, Bokun Wang, Jianling Wang, Xiangjue Dong, Tianbao Yang, James Caverlee  
Department of Computer Science and Engineering, Texas A&M University  
liuhr99,bokun-wang,jlwang,xj.dong,tianbao-yang,caverlee@tamu.edu

## ABSTRACT

As powerful tools for representation learning on graphs, graph neural networks (GNNs) have played an important role in applications including social networks, recommendation systems, and online web services. However, GNNs have been shown to be vulnerable to adversarial attacks, which can significantly degrade their effectiveness. Recent state-of-the-art approaches in adversarial attacks rely on gradient-based meta-learning to selectively perturb a single edge with the highest attack score until they reach the budget constraint. While effective in identifying vulnerable links, these methods are plagued by high computational costs. By leveraging continuous relaxation and parameterization of the graph structure, we propose a novel attack method called Differentiable Graph Attack (DGA) to efficiently generate effective attacks and meanwhile eliminate the need for costly retraining. Compared to the state-of-the-art, DGA achieves nearly equivalent attack performance with 6 times less training time and 11 times smaller GPU memory footprint on different benchmark datasets. Additionally, we provide extensive experimental analyses of the transferability of the DGA among different graph models, as well as its robustness against widely-used defense mechanisms.

## KEYWORDS

graph neural networks; adversarial attack; gray-box attack

### ACM Reference Format:

Haoran Liu, Bokun Wang, Jianling Wang, Xiangjue Dong, Tianbao Yang, James Caverlee. 2018. Everything Perturbed All at Once: Enabling Differentiable Graph Attacks. In *Proceedings of Make sure to enter the correct conference title from your rights confirmation email (Conference acronym 'XX)*. ACM, New York, NY, USA, 15 pages. <https://doi.org/XXXXXXXX.XXXXXX>

## 1 INTRODUCTION

Graph Neural Networks (GNNs) [17, 24] are powerful in modeling graph-structured data and show remarkable performance on many real-world applications such as social networks [11, 39, 46], recommendation systems [5, 36, 52, 58, 61], and drug discovery [19, 41]. Given the successful applications of GNNs, there are also growing concerns about their robustness under adversarial attacks [3, 7, 33, 51, 67]. For example, toxic behavior detectors with GNN backbones

could be vulnerable to adversarial attacks, leading to undetected instances of harassment, extremism, or radicalization targeting innocent individuals on social media [8, 18]. To ensure the reliability and safety of GNN-based systems in practice, it becomes paramount to understand their vulnerabilities to adversarial attacks as a foundation for their robust deployment. In a nutshell, developing more effective adversarial attack methods on GNNs not only aids in assessing the robustness and defense strategies of GNNs [14, 20, 45, 59, 60, 63] but also enhances the understanding of the underlying properties of current GNN models.

Presently, adversarial attacks on GNNs can be categorized based on the attacker's capacity, goal, level of knowledge, and perturbation type [21, 42, 56]. One of the most practical setups among these is the **gray-box attack**, in which attackers have complete knowledge of the training data but no information on the victim model. Following this setup as in previous works [29, 30, 67], within the budget limit, we seek for attacking strategies which perform topology attacks (*i.e.* adding or removing edges) on poisoning training data to compromise the overall node classification performance of the victim model.

Despite the effectiveness in identifying vulnerable edges via the gradient-based “*learn to attack*” approaches, the state-of-the-art methods [30, 67] in graph adversarial attacks are faced with two major bottlenecks: (i) **Non-convexity and discrete structure**: Meta-learning approaches usually formulate the attack as a bi-level optimization problem, which is challenging to solve due to the non-convexity of both levels, making it difficult to derive a closed-form solution. Additionally, the discrete nature of the graph structure poses another challenge for directly applying widely-used gradient-based techniques such as FGSM [16] and PGD [34], which are typically employed on image data; and (ii) **Computational and resource costs**: Existing methods selectively perturb a single edge with the highest attack score and require retraining the surrogate model from scratch, incurring high computational costs. Additionally, it is unrealistic to scale these techniques to handle large datasets.

To tackle the above-mentioned bottlenecks, we propose the **Differentiable Graph Attack** (DGA) with continuous relaxation on the graph structure. It offers several advantages with its novel *train-then-sample* attack scheme. During the training process, instead of searching over a discrete set of candidate perturbations, we *relax* the search space to a continuous space, so that the graph structure can be optimized with respect to the attack objective through gradient descent, allowing for fine-grained adjustments and improved effectiveness of the attack. Then, we simulate the lower-level optimization process with one-step fine-tuning on the surrogate model to avoid calculating the accumulation of meta-gradients and further reduce computation complexity. This offers

Permission to make digital or hard copies of all or part of this work for personal or classroom use is granted without fee provided that copies are not made or distributed for profit or commercial advantage and that copies bear this notice and the full citation on the first page. Copyrights for components of this work owned by others than ACM must be honored. Abstracting with credit is permitted. To copy otherwise, or republish, to post on servers or to redistribute to lists, requires prior specific permission and/or a fee. Request permissions from [permissions@acm.org](mailto:permissions@acm.org).

Conference acronym 'XX, June 03–05, 2018, Woodstock, NY

© 2018 Association for Computing Machinery.  
ACM ISBN 978-1-4503-XXXX-X/18/06...\$15.00  
<https://doi.org/XXXXXXXX.XXXXXX>

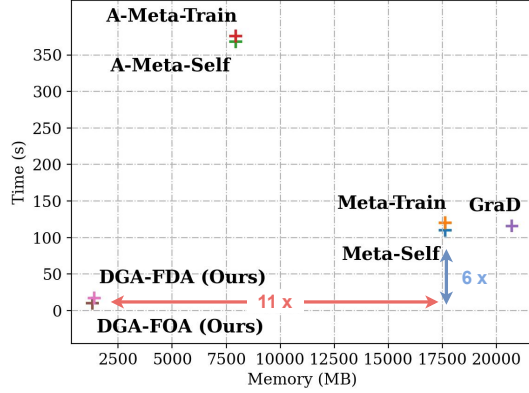


**Figure 1: Comparison on computation and resource complexity between MetAttack [67], GraD [30] and two variants of our DGA method on CiteSeer with 5% perturbation rate.**

more control over the attack process compared to methods with fixed attack epochs. Essentially, DGA utilizes a single-step adaption approach to simulate the poisoning process, offering a trade-off between the poisoning simulation procedure and training time. For the sampling stage, our sampling scheme enables DGA to generate poisoned graphs with varying budgets while being trained only once, further streamlining the attack process. Theoretically, we show that the estimation error in forward/backward passes of our algorithm, as well as the convergence of the method, depends on the error of edge sampling. These benefits collectively make DGA a powerful and efficient method for generating adversarial attacks on graph structures, as shown in Figure 1. “FOA” and “FDA” refer to first-order approximation and finite-difference approximation, respectively (See Section 3.1 for details).

We conduct empirical analysis of DGA with common benchmark datasets. Our main contributions are summarized as follows:

- **Effectiveness.** DGA outperforms or performs comparably to the SOTA methods on widely-used datasets. Notably, our method is effective even when the perturbation budget is low, which is more aligned with real-world scenarios and maintains the unnoticeability of the attack.
- **Time and Resource Efficiency.** DGA is more than 6 times faster and requires approximately 11 times less GPU memory than SOTA methods. Importantly, the attack time of DGA remains constant even as the perturbation budget increases. Additionally, DGA can be easily adapted to large-scale graphs, making it a practical choice for real-world scenarios.
- **Transferability and Imperceptibility.** DGA exhibits excellent transferability to a variety of GNN models and demonstrates imperceptibility toward commonly-used defense methods. These findings highlight the valuable role of DGA in assessing the robustness of existing GNN methods and providing insights for the development of novel defense strategies against adversarial attacks.

## 2 BACKGROUND

We consider the task of semi-supervised node classification, in which a model is trained to predict the labels of nodes in a graph, using both labeled and unlabeled data. We denote an undirected graph as  $G = (\mathcal{V}, \mathcal{E})$ , where  $\mathcal{V} = \{i = 1, \dots, N\}$  is the set of  $N$  nodes, and  $\mathcal{E} \subseteq \mathcal{V} \times \mathcal{V}$  is the edge set with cardinality  $|\mathcal{E}| = M$ . In the semi-supervised setting, we are given a subset  $\mathcal{V}_L \subseteq \mathcal{V}$  of labeled nodes, in which the nodes are associated with class labels from  $C = \{c_1, c_2, \dots, c_k\}$ . The goal is to learn a function  $f$  to infer labels of nodes in the unlabeled node set  $\mathcal{V}_U = \mathcal{V} \setminus \mathcal{V}_L$ . Without loss of generality, we collectively use  $X \in \mathbb{R}^{N \times D}$  to denote the node features of all nodes in the graph, where  $D$  is the dimension of feature vectors. Additionally, we denote the adjacency matrix associated with this graph as  $A \in \{0, 1\}^{N \times N}$ . For each entry  $(i, j)$  in  $A$ ,  $A_{i,j} = 1$  if  $(i, j) \in \mathcal{E}$  and 0 otherwise. In this context, the neighborhood of node  $v$  is denoted as  $\mathcal{N}(v) = \{i \in \mathcal{V} : (i, v) \in \mathcal{E}\}$ . Given a graph  $G$ , the node embeddings are obtained by using a GNN model  $f_\theta(X, A)$ , parameterized by  $\theta$ . Particularly, the GNN model takes the node features  $X$  and adjacency information  $A$  as input and outputs the logits of each node.

### 2.1 Problem Setting

We follow [67] and focus on the *combination* of the following specific attack setting: (1) **gray-box**, in which the attackers have access to complete information about the training data but zero knowledge about the specifics of the underlying model. To overcome this challenge, surrogate models are utilized to approximate and simulate the behavior of the target model; (2) **poisoning**, in which the attacker’s goal is to increase the classification error (*i.e.* one minus accuracy) by training on modified (*i.e.* poisoned) data; (3) **graph structure attack**, in which the attacker’s perturbation type is adding/removing edges. To ensure the attack remains undetected, a maximum perturbation budget denoted as  $\Delta$ , which restricts the difference between the perturbed graph structure  $A$  and the original structure  $A_{orig}$  such that  $\|A - A_{orig}\|_0 \leq 2\Delta$ ; (4) **untargeted/global**, in which the attacker’s goal is to compromise the *overall* node classification performance of the model instead of targeting individual nodes.

Formally, this specific graph attack setting can be formulated as a *bi-level optimization* problem

$$\begin{aligned} \min_{A \in \mathcal{A}_\Delta} \quad & \ell_{atk}(f_{\theta^*}(X, A), Y), \\ \text{s.t.} \quad & \theta^* = \arg \min_{\theta} \ell_{train}(f_{\theta}(X, A), Y), \end{aligned} \quad (1)$$

where  $\mathcal{A}_\Delta := \{A' \in \{0, 1\}^{N \times N} \mid \|A' - A_{orig}\|_0 \leq 2\Delta\}$  denotes the search space containing all possible adjacency matrices with the given modification budget  $\Delta$ . Here, the upper-level optimization aims to find the optimal edge perturbations which result in a new adjacency matrix  $A$  that maximizes the attack success. The attack objective  $\ell_{atk}$  could be the inverse of either training loss  $\ell_{train}$  or self-training loss  $\ell_{self}$ . Specifically,  $\ell_{train}$  is the cross-entropy loss on the training set and  $\ell_{self}$  is computed with pseudo labels for the unlabeled nodes. The pseudo labels are predicted by a well-trained surrogate model given the clean graph. In a sense,  $\ell_{self}$  can be used to estimate the generalization loss after the attack. As for the nested inner problem, the lower-level optimization targets finding

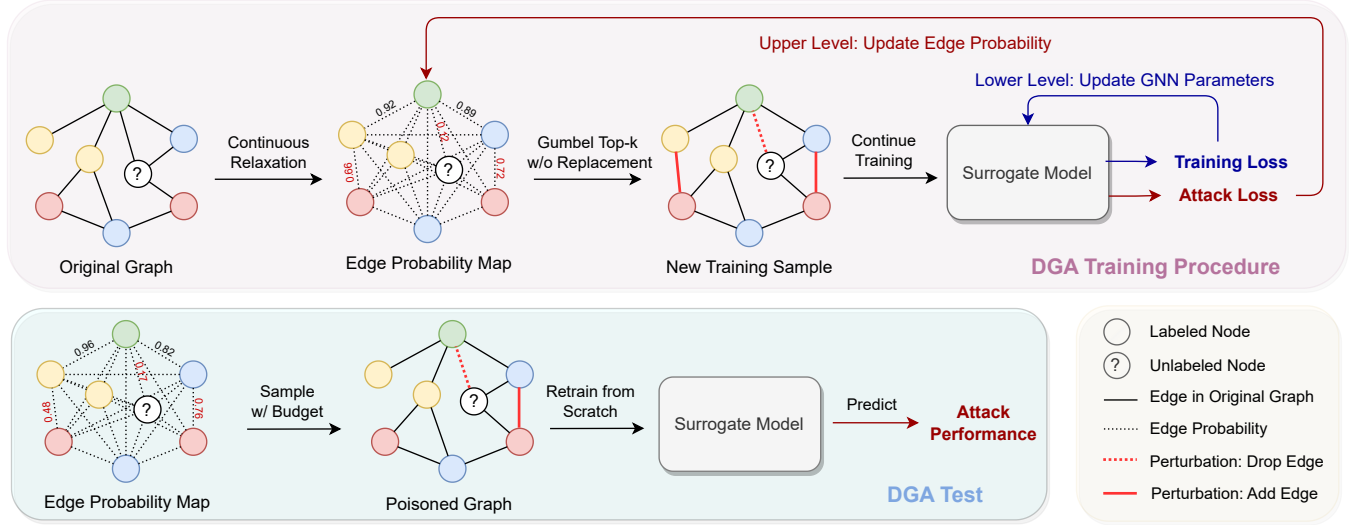


Figure 2: Illustration of the DGA framework. Node colors indicate different classification labels.

the optimal GNN parameters  $\theta^*$  through an optimization process of training the GNN on the perturbed graph from scratch. Essentially, finding a good attack method for GNNs involves solving this bi-level optimization problem in a effective and efficient manner.

### 3 DIFFERENTIABLE GRAPH ATTACK

In light of the non-convex and combinatorial characteristics of the optimization problem presented in Equation (1), it is infeasible to acquire a closed-form solution or employ gradient-based iterative algorithms commonly used in deep learning. To address this challenge, we propose a novel approach that is both effective and efficient by continuous relaxing and parameterizing the graph structure as a continuous edge probability map. An illustration of the DGA framework is shown in Figure 2.

#### 3.1 Continuous Relaxation on Graph Structure

We model each edge with a Bernoulli random variable and transform the discrete graph adjacency matrix  $A$  to an unnormalized probability matrix  $P$ , where the  $(i, j)$ -th element  $p_{ij}$  indicates the (unnormalized) edge probability between node  $i$  and node  $j$  under the attack setting. Then, the search space for modified adjacency matrix  $\{0, 1\}^{N \times N}$  is relaxed to the positive orthant  $\mathbb{R}_{++}^{N \times N}$ . As shown in Figure 2, there is no need to enforce the perturbation budget constraint during the DGA training process. The technique outlined in Section 3.3 ensures that the generated poisoned graph consistently adheres to the budget. We consider the following continuous relaxation of (1).

$$\begin{aligned} & \min_{P \in \mathbb{R}_{++}^{N \times N}} \ell_{atk}(f_{\theta^*}(X, P), Y), \\ \text{s.t. } & \theta^* = \underset{\theta}{\operatorname{argmin}} \ell_{train}(f_{\theta}(X, P), Y). \end{aligned} \quad (2)$$

Instead of exactly solving the lower-level problem, we approximate the optimal surrogate model  $\theta^*$  by a single-step adaptation with step size  $\alpha$  following the techniques in Finn et al. [13], Liu et al. [27]. By changing variables  $Q = \log P$ , the optimization problem

in (2) becomes unconstrained w.r.t. unnormalized log-probabilities  $Q$ . We define that  $\mathbf{q} := \operatorname{vec}(Q)$ ,  $\mathcal{L}_{atk}(\theta, \mathbf{q}) := \ell_{atk}(f_{\theta}(X, P), Y)$ ,  $\mathcal{L}_{train}(\theta, \mathbf{q}) := \ell_{train}(f_{\theta}(X, P), Y)$ , and  $\nabla_1 \mathcal{L}(\cdot, \cdot)$ ,  $\nabla_2 \mathcal{L}(\cdot, \cdot)$  are gradients of  $\mathcal{L}$  with respect to its first and second arguments, respectively. Then, the bi-level optimization in (2) becomes a simpler compositional optimization problem.

$$\min_{\mathbf{q} \in \mathbb{R}^{N \times N}} \mathcal{L}_{atk}(\hat{\theta}, \mathbf{q}), \quad \hat{\theta} = \theta - \alpha \nabla_{\theta} \mathcal{L}_{train}(\theta, \mathbf{q}). \quad (3)$$

The hyper-gradient with respect to the log probabilities  $\mathbf{q}$  can be computed as

$$\nabla_{\mathbf{q}} \mathcal{L}_{atk}(\hat{\theta}, \mathbf{q}) = \nabla_2 \mathcal{L}_{atk}(\hat{\theta}, \mathbf{q}) - \alpha \nabla_{1,2}^2 \mathcal{L}_{train}(\theta, \mathbf{q}) \nabla_1 \mathcal{L}_{atk}(\hat{\theta}, \mathbf{q}). \quad (4)$$

Based on the hyper-gradient, we can update the log-probability matrix  $Q$  by a gradient descent step. It is worth noting that the Hessian matrix computation in (4) can be costly when the number of nodes is large. To this end, we can either set  $\alpha = 0$  in the hyper-gradient (“first-order approximation”) or use the finite difference approximation similar to Liu et al. [27]. To be specific, with  $\theta_{\pm} = \theta \pm \delta \nabla_1 \mathcal{L}_{atk}(\hat{\theta}, \mathbf{q})$ , we can approximate the last term in (4) as

$$\nabla_{1,2}^2 \mathcal{L}_{train}(\theta, \mathbf{q}) \nabla_1 \mathcal{L}_{atk}(\hat{\theta}, \mathbf{q}) \approx \frac{\nabla_2 \mathcal{L}_{train}(\theta_+, \mathbf{q}) - \nabla_2 \mathcal{L}_{train}(\theta_-, \mathbf{q})}{2\delta}.$$

In the rest of the paper, we refer to the variant of our algorithm using first-order approximation ( $\alpha = 0$  in Eq. 4) as **DGA-FOA**, and the variant using the finite difference approximation as **DGA-FDA**.

#### 3.2 Edge Sampling for Expressiveness and Efficiency

Note that the gradient-based continuous optimization of (3) results in a dense probability matrix  $P$ . Utilizing this matrix as input may lead to over-smoothing [17, 62] or over-squashing [9] of the surrogate graph neural network  $\theta$ . Moreover, message passing on a dense graph exacerbates the issue of “neighborhood explosion”, which significantly increases computational costs. To resolve this problem,

**Algorithm 1** Training Procedure of Differentiable Graph Attack (DGA)

- 
- 1: **Input:** Graph structure  $A_{orig}$ , step size  $\eta$ , total num. of iterations  $T$ , node features  $X$ , labels  $Y$
  - 2: **Initialize:**  
 $Q_0 \leftarrow \log(A_{orig} + \epsilon)$  ▷ Add an  $\epsilon$  to avoid numerical issue  
 $\theta \leftarrow \operatorname{argmin}_{\theta} \ell_{train}(f_{\theta}(X, A_{orig}), Y)$
  - 3: **for**  $t = 0, 1, \dots, T - 1$  **do**
  - 4:   Sample a sparse graph  $\tilde{A}_t$  from unnormalized log-probabilities  $Q_t$  by Gumbel top- $k$  sampling
  - 5:   Compute the single-step adaptation by  $\hat{\theta}_t = \theta - \alpha \nabla_{\theta} \ell_{train}(f_{\theta}(X, \tilde{A}_t), Y)$
  - 6:   Compute the approximated hyper-gradient  $\tilde{\nabla}_t$  based on  $\hat{\theta}_t$  and  $\tilde{A}_t$ : Option I: first-order approximation (FOA) or Option II: finite-difference approximation (FDA)
  - 7:   Update the probability matrix by  $Q_{t+1} = Q_t - \eta \tilde{\nabla}_t$  and symmetrize  $Q_{t+1}$
  - 8: **end for**
  - 9: Obtain the probability matrix  $P$  from the unnormalized log-probability matrix  $Q_T$
  - 10: **Return:** Probability matrix  $P$  for graph poisoning
- 

we use the Gumbel-Top- $k$  trick [25, 55] to sample a sparser graph  $\tilde{A}$  from the unnormalized log-probabilities  $Q$ . Formally, for the  $i$ -th node  $v_i$ , we construct  $k$  edges between  $v_i$  and each of the first  $k$  elements of

$$\operatorname{argsort}_j(-\log(-\log(u_j)) + Q_{ij}),$$

where  $u_j$  is a vector randomly sampled from the uniform distribution. The top- $k$  operation can be replaced by the differentiable relaxed top- $k$  operation in Xie and Ermon [55]. Intuitively, such sampling can be regarded as a stochastic relaxation of the  $k$ -nearest neighbors rule.

### 3.3 Obtaining the Poisoned Graph

Utilizing the learned edge probability map  $P$  (output of Alg. 1), we generate perturbations by sampling from the discrepancy between the final and initial edge probability maps. This process serves to test the performance of the DGA attack, as illustrated in the blue box in Figure 2. To prepare for the attack, DGA first symmetrizes the edge probability matrix  $P$  for undirected graphs as  $\tilde{P} = \frac{1}{2}(P + P^T)$ . Next, we compute the difference score matrix  $S = (\tilde{P} - A_{orig}) \odot (1 - 2A_{orig})$ , where  $\odot$  indicates element-wise multiplication. Here we flip the sign of difference score for every connected edge in the original graph  $A_{orig}$ , which allows us to identify existing edges with the most significant negative impact, as well as the non-existent edges with the most potent positive influence on the attack objective. The resulting difference score matrix  $S$  is employed to construct a categorical distribution, from which we can sample perturbations in order to obtain the poisoned graph.

Taking into account the allocated attack budget, we sample  $\Delta$  edges from the categorical distribution without replacement and flip them, thereby generating a poisoned graph. Subsequently, we proceed to train models from scratch using this poisoned graph, allowing us to assess the attack's performance on a specific model.

In practice, we repeat this sampling process multiple times and select the instance that yields the best  $\ell_{atk}$  (attack loss) value.

## 4 CONVERGENCE ANALYSIS

Before the  $t$ -th iteration, our algorithm samples edges for each node  $i$  by the Gumbel top- $k$  trick, which is equivalent to sampling  $k$  edges from  $\mathbf{p}_t^i = (p_t^{i,1}, \dots, p_t^{i,N})$  without replacement [25], where  $\mathbf{p}_t^i$  is the normalized probabilities corresponding to the  $i$ -th line of  $Q_t$ . This result in the sparsified log-probability matrix  $\tilde{Q}_t = \operatorname{Diag}(\tilde{\mathbf{q}}_t)$  and  $\tilde{\mathbf{q}} \in \{0, 1\}^{N^2}$  is a vector that stores sampled edges for each node, i.e.  $\tilde{\mathbf{q}}_t^{i,j} = \mathbf{q}_t^{i,j}$  if the edge  $(i, j)$  is sampled and  $\tilde{\mathbf{q}}_t^{i,j} = 0$  otherwise. Note that the sampled adjacency matrix  $\tilde{A}_t$  is just the binarized copy of  $\tilde{Q}_t$ . For brevity, we define that  $\Phi(\mathbf{q}) := \mathcal{L}_{atk}(\hat{\theta}, \mathbf{q})$ ,  $\hat{\theta} = \theta - \alpha \nabla_{\theta} \mathcal{L}_{train}(\theta, \mathbf{q})$ . We make some regularity assumptions of the loss functions.

**Assumption 1.** Suppose that the loss function  $\mathcal{L}_{atk}$  is Lipschitz continuous and has Lipschitz-continuous gradient while  $\mathcal{L}_{atk}$  has Lipschitz continuous gradient and Hessian.

**Lemma 1.** Under Assumption 1, there exists  $G > 0$  and  $L > 0$  such that  $\Phi$  is  $G$ -Lipschitz continuous and  $\nabla\Phi$  is  $L$ -Lipschitz continuous.

The proof of Lemma 1 can be found in Appendix A. With the sparsified  $\tilde{\mathbf{q}}$ , we approximate the objective function  $\Phi(\mathbf{q})$  by  $\Phi(\tilde{\mathbf{q}})$  and the error is

$$\|\Phi(\tilde{\mathbf{q}}_t) - \Phi(\mathbf{q}_t)\|_2 \leq G \|\tilde{\mathbf{q}}_t - \mathbf{q}_t\|_2, \quad (5)$$

where  $\|\tilde{\mathbf{q}}_t - \mathbf{q}_t\|_2$  is the estimation error by cause of the edge sampling per iteration. Besides, the hyper-gradient  $\nabla\Phi(\mathbf{q})$  in (4) can be estimated by

$$\begin{aligned} \nabla\Phi(\tilde{\mathbf{q}}) &= \nabla_2 \mathcal{L}_{atk}(\hat{\theta}, \tilde{\mathbf{q}}) - \alpha \nabla_{1,2}^2 \mathcal{L}_{train}(\theta, \tilde{\mathbf{q}}) \nabla_1 \mathcal{L}_{atk}(\hat{\theta}, \tilde{\mathbf{q}}), \\ \hat{\theta} &= \theta - \alpha \nabla_{\theta} \mathcal{L}_{train}(\theta, \tilde{\mathbf{q}}), \end{aligned}$$

where  $\nabla\Phi(\tilde{\mathbf{q}})$  is the vectorized  $\tilde{\nabla}_t$  in Alg. 1. Next, we present the main theorem on convergence.

**Theorem 2.** Under assumptions above, our algorithm with proper step size  $\eta$  leads to

$$\mathbb{E} \|\nabla\Phi(\mathbf{q}_\tau)\|_2^2 \leq \mathcal{O} \left( \frac{\Phi(\mathbf{q}_0) - \inf_{\mathbf{q}} \Phi}{T} + \operatorname{Avg.Err.} \right), \quad (6)$$

where  $\tau$  is sampled from  $\{0, 1, \dots, T - 1\}$  uniformly at random and  $\operatorname{Avg.Err.}$  is the average error due to edge sampling across the iterations. To be specific,  $\operatorname{Avg.Err.} := \frac{1}{T} \sum_{t=0}^{T-1} \mathbb{E} \|\tilde{\mathbf{q}}_t - \mathbf{q}_t\|_2^2$ .

**Remark 1.** The proof of Theorem 2 can be found in Appendix A. Theorem 2 demonstrates that our algorithm exhibits an  $\mathcal{O}(1/T)$  non-asymptotic convergence rate when  $k = N$ , the same as that of gradient descent. While opting for a larger value of  $k$  can be advantageous from the estimation/optimization perspective, it results in worse expressiveness and efficiency as explained in Section 3.2. Therefore, we can manage the trade-off between estimation/optimization error and expressiveness/efficiency by adjusting the hyper-parameter  $k$ . Fortunately, the estimation error  $\|\tilde{\mathbf{q}}_t - \mathbf{q}_t\|_2$  could be negligible even with a small  $k$  when the distribution constructed by  $\mathbf{p}_i$  is light-tailed (e.g., power law), thanks to the Gumbel top- $k$  sampling.

**Table 1: Dataset statistics.**

Dataset	#Nodes	#Edges	#Classes	#Features	# Avg. Deg.
Citeseer	2,110	3,757	6	3,703	1.43
Cora	2,485	5,069	7	1,433	2.00
PolBlogs	1,222	16,714	2	–	13.68

## 5 EXPERIMENTS

Our proposed attack method, DGA (Differentiable Graph Attack), is evaluated through a series of experiments aimed at demonstrating its effectiveness and efficiency. The experimental settings are introduced in Section 5.1. The attack performance and the generalizability and transferability of DGA is analyzed in Section 5.2. We also show the computation complexity of DGA in Section 5.3. Furthermore, we conduct experiments with defense methods in Section 5.4 to demonstrate the robustness of our approach. Additionally, we present a study on Gumbel- $k$  in Section 5.5 and provide visualization of the distribution of the generated poisoned graph in Section 5.6.

### 5.1 Experimental Settings

**Dataset.** The experiments are conducted on three widely-used datasets: two citation network datasets, namely CiteSeer [40] and Cora [35], and one social network dataset PolBlogs [1]. All experiments are performed on the largest connected component of the graphs. Following previous works [20, 66], we randomly split the datasets into the train, validation, and test sets using a 10%, 10%, and 80% ratio, respectively. For each experiment, we report the average performance of 10 runs. The experiments are conducted on the largest connected component (LCC) of the graphs, ensuring that only the main connected portion of the graphs is considered for analysis and evaluation. The statistics for the LCC of these datasets are summarized in Table 1.

**Victim Models.** Following previous methods, we first take the widely-used GCN [24] as our victim model. Moreover, as we adopt a gray-box setting, in which the model architecture is considered unknown, we further conduct experiments with Graph Attention Network (GAT) [48] and DeepWalk [38] to measure the transferability of DGA. Additionally, to assess the effectiveness of our proposed DGA attack method, we conduct experiments to evaluate its robustness against existing defense methods, namely GCN-Jaccard and GCN-SVD.

**Perturbation Budgets.** To be closer to real-world scenarios and demonstrate the imperceptibility of the attack method, we set 1%, 3%, and 5% as the perturbation budget in our experiments. Each method is allowed to modify 1%, 3%, and 5% of the number of edges in the original graph, respectively.

**Baselines.** To assess the effectiveness and applicability of DGA, we conduct a comprehensive comparison with six representative baselines: including heuristic-based method DICE [53] and learning-based methods Meta-Self, Meta-Train, A-Meta-Self, A-Meta-Train [67], and GraD [30].

Additional information about the experimental setup, implementation, and baselines can be found in Appendix B. <sup>1</sup>

<sup>1</sup>The code will be made publicly available once accepted.

### 5.2 Attack Performance

Table 2 presents the test accuracy results of the proposed DGA method compared to baselines. The accuracy values for the original clean graphs are reported under the 0% perturbation rate column. Remarkably, DGA outperforms or closely approximates the best performance in 8 out of 9 metrics, while exhibiting a significantly reduced training time (over 6 times faster) and GPU memory usage (over 11 times less) compared to the previous SOTA Meta-Self and Meta-Train methods. Additionally, DGA demonstrates strong attack performance even at low perturbation rates, causing a mere 3% to 4% drop in test accuracy with only a 1% budget. Notably, the DGA-FOA method consistently achieves better results than its counterpart, DGA-FDA, on 7 out of 9 metrics. This observation suggests that the first-order approximation exhibits greater robustness and efficacy in practical applications. Detailed descriptions and reproduction information for these baselines can be found in Appendix B.4. Note that the GraD paper [30] evaluates their performance on the overall graph, distinct from the commonly used LCC setting. Standard deviations of these experiments are provided in Appendix C.1.

**Generalizability and Transferability.** In order to be consistent with the gray-box attack setting, in which attackers have no information on the victim model, we evaluate the generalizability and transferability of DGA with two different GNN models. We conduct experiments with both supervised attention-based method GAT [48] and unsupervised random walk-based method DeepWalk [38] trained with the DGA poisoned graph. These graphs are derived using GCN as the surrogate model. Detailed descriptions for these base models are provided in Appendix B.3. The results, shown in the GAT and DeepWalk section in Table 4, demonstrate that our method achieves good transferability performance on both GAT and DeepWalk models. Our method achieved the best or second-best performance in 11 out of 18 metrics. Note that since the graph poisoned by DICE contains isolated nodes, we do not evaluate DeepWalk with this method.

### 5.3 Training Time and Memory Usage.

Table 3 presents a comparison of training time and maximum GPU memory usage between the proposed DGA method and baselines, considering a 5% perturbation rate. Our approach demonstrates significantly shorter training time and lower memory usage compared to the baselines. Regarding training time, our DGA methods demonstrate significant efficiency. Specifically, when compared to the previous SOTA methods, DGA achieves training time reductions of over 5, 6, and 16 times on the Citeseer, Cora, and PolBlogs datasets, respectively. Furthermore, our DGA methods exhibit superior efficiency in terms of GPU memory usage. Compared to the SOTA methods, DGA showcases reductions of over 11, 12, and 15 times on the Citeseer, Cora, and PolBlogs datasets, respectively. Additional comparisons with other budgets can be found in Appendix C.2. It is worth noting that DICE is a random perturbation method that runs quickly and does not utilize GPU resources. These findings highlight the computational advantages of DGA, making it a highly efficient and scalable solution for adversarial attacks on graph structures. The substantial reductions in training time and GPU memory usage signify the potential of DGA for practical

**Table 2: Test accuracy (%) of the GCN model after training with clean and poisoned graphs. The average performance are calculated based on 10 runs. The top-two results are highlighted as 1st (bold) and 2nd (underlined). The standard deviations are provided in Appendix C.**

Dataset Perturbation Rate (%)	CiteSeer				Cora				PolBlogs			
	0	1	3	5	0	1	3	5	0	1	3	5
DICE [53]	71.81	71.40	70.73	70.05	83.62	82.43	81.96	81.45	95.00	92.41	89.29	86.85
Meta-Self [67]	71.81	71.48	69.3	<b>66.91</b>	83.62	82.08	<u>78.88</u>	<b>75.46</b>	95.00	<b>85.02</b>	<b>79.17</b>	<b>76.40</b>
Meta-Train [67]	71.81	70.50	69.31	67.86	83.62	82.16	79.99	77.69	95.00	92.42	88.85	88.46
A-Meta-Self [67]	71.81	71.29	70.83	69.97	83.62	83.32	82.45	81.69	95.00	94.30	92.90	92.16
A-Meta-Train [67]	71.81	70.60	69.02	67.54	83.62	82.18	79.24	77.12	95.00	94.39	92.10	90.45
GraD [30]	71.81	71.64	70.88	70.66	83.62	83.43	82.77	82.29	95.00	91.77	89.01	88.71
DGA-FOA (ours)	71.81	<u>68.75</u>	<b>67.89</b>	<b>66.91</b>	83.62	<b>79.89</b>	<b>78.77</b>	<u>78.07</u>	95.00	91.31	<u>88.45</u>	<u>87.01</u>
DGA-FDA (ours)	71.81	<b>68.51</b>	<u>68.15</u>	<u>67.45</u>	83.62	<u>81.16</u>	80.32	79.50	95.00	<u>90.90</u>	89.26	87.63

applications in real-world scenarios, as it can be easily applied to large-scale graphs.

#### 5.4 Robustness against Existing Defense Methods

To evaluate the effectiveness of our proposed DGA attack method, we conduct experiments to test its robustness against existing defense methods. By doing so, we aim to assess whether our attack method could overcome these defense methods and reveal vulnerabilities in the system that were previously undiscovered. We test DGA against two popular defense methods, namely GCN-Jaccard [57] and GCN-SVD [10]. Detailed descriptions for these defense models are provided in Appendix B.3. In these experiments, the poisoned graphs are first vaccinated with defense models. Then a GCN model is trained from scratch on the vaccinated graph. We report the classification accuracy of the well-trained GCN model. Results are shown in the Low-rank SVD and Jaccard section in Table 4. Note that we cannot perform Jaccard on the PolBlogs dataset, as this dataset does not contain node features. Our method achieves the best or second-best performance compared with the baseline on 11 out of 15 metrics. These results demonstrate the effectiveness of our DGA attack method in overcoming existing defense methods and exposing potential vulnerabilities of GNN models.

**Table 3: Comparison of training time (in seconds), GPU memory occupancy (in MB) after attack between DGA and baselines with 5% perturbation rate. All experiments are conducted on a single 24GB NVIDIA RTX A5000 GPU for a fair comparison.**

Dataset Method	Citeseer		Cora		PolBlogs	
	Time	Mem.	Time	Mem.	Time	Mem.
Meta-Self [67]	114	17,629	172	21,993	225	18,453
Meta-Train [67]	114	17,629	172	21,993	225	18,453
A-Meta-Self [67]	368	7,933	692	13,375	462	12,289
A-Meta-Train [67]	376	7,933	692	13,375	462	12,289
GraD [30]	116	20,723	176	23,515	138	19,163
DGA-FOA (ours)	<b>14</b>	<b>1,327</b>	<b>15</b>	<b>1,563</b>	13	<b>1,109</b>
DGA-FDA (ours)	17	1,365	24	1,635	<b>8</b>	1,129

#### 5.5 Impact of Gumbel- $k$

In this section, we conduct ablation studies on the hyperparameter  $k$  for the Gumbel- $k$  trick in DGA-FOA using the Cora dataset. As shown in Table 5, the performance of DGA remains relatively stable across different perturbation rates for varying values of "k." However, we observe a trend where the performance first improves and then declines as  $k$  increases. Increasing  $k$  initially enhances DGA's performance, indicating its potential for better results. Nevertheless, we find that beyond a certain threshold, the performance starts to decline. This drop in performance can be attributed to overfitting and over-squashing of the GNNs. When  $k$  becomes excessively large, the graph becomes dense and closely resembles a fully-connected graph, leading to over-squashing and reduced generalization. Notably, the average degree of the dataset is around 2, as indicated in Table 1. The ablation study highlights that the best-performing DGA configurations are achieved when setting  $k$  around the average degree of the dataset. While higher  $k$  values may improve DGA's ability to exploit complex structures, they come at the cost of increased computational resources. Hence, we suggest choosing  $k$  near the average degree of the graph to achieve a good balance between performance and computational efficiency.

#### 5.6 Visualization and Analysis of DGA Attacked Graphs

To elucidate the impact of the attack on the graph structure and its implications for the performance and behavior of the targeted model, we visualize three properties for the clean graph and poisoned graph on the Citeseer dataset, as shown in Figure 3. Additional visualizations on other datasets are provided in Appendix C.3. Firstly, the node degree distributions for the clean graph and perturbed graph are shown in Figure 3a. Notably, we observe that the degree distributions of the two graphs exhibit high similarities. This observation provides evidence for the imperceptibility of our proposed DGA attack. Furthermore, we present the feature similarity and label equality analysis for different types of edges in the graphs, as shown in Figure 3b and Figure 3c, respectively. We can observe that DGA exhibits a tendency to establish connections between nodes that possess dissimilar features and have different labels while removing edges that link nodes sharing similar features and belonging to the same label. These observations align with the

**Table 4: An evaluation of DGA in generalizability, transferability, and robustness against existing defense methods. The first two sections show the test accuracy (%) of GAT [48] and DeepWalk [38] models trained with both clean and poisoned graphs, where the surrogate model is GCN. The last two sections show the test accuracy (%) of GCN models trained with clean and poisoned graphs and subsequently vaccinated with two commonly-used defense mechanisms, namely low-rank SVD approximation [10] (GCN-SVD) and Jaccard (GCN-Jaccard) [57]. To ensure comprehensive evaluation, we conduct 10 runs of experiments and report the average performance. The top-two results are highlighted as 1st (bold) and 2nd (underlined). The standard deviations are provided in Appendix C. Note that we cannot perform Jaccard on PolBlogs, as this dataset does not contain node features.**

Victim Model	Dataset Perturbation Rate (%)	CiteSeer				Cora				PolBlogs			
		0	1	3	5	0	1	3	5	0	1	3	5
GAT [48]	DICE [53]	73.51	73.71	<b>72.67</b>	72.18	84.06	84.09	83.45	82.92	94.97	93.81	92.12	<b>90.97</b>
	Meta-Self [67]	73.51	73.87	73.98	73.42	84.06	83.85	83.52	83.60	94.97	<u>93.27</u>	92.33	91.57
	Meta-Train [67]	73.51	73.64	74.19	73.87	84.06	83.93	83.96	83.27	94.97	93.88	<b>91.57</b>	91.81
	A-Meta-Self [67]	73.51	73.05	72.71	72.32	84.06	83.97	83.34	<b>82.11</b>	94.97	93.91	92.44	<u>91.10</u>
	A-Meta-Train [67]	73.51	73.96	73.86	73.15	84.06	84.08	83.37	82.84	94.97	94.58	93.93	93.10
	GrAD [30]	73.51	<u>72.95</u>	74.16	73.23	84.06	84.22	83.63	83.03	94.97	<b>92.96</b>	<u>92.11</u>	91.70
	DGA-FOA (ours)	73.51	73.44	<u>72.86</u>	<u>71.94</u>	84.06	<u>83.60</u>	<u>83.33</u>	82.79	94.97	93.84	93.33	92.56
	DGA-FDA (ours)	73.51	<b>72.86</b>	73.15	<b>71.73</b>	84.06	<b>83.38</b>	<b>82.46</b>	<u>82.43</u>	94.97	93.93	93.11	91.27
DeepWalk [38]	Meta-Self [67]	69.79	70.23	69.36	69.54	79.11	78.90	78.48	78.19	95.51	<b>93.59</b>	<u>92.83</u>	<u>92.15</u>
	Meta-Train [67]	69.79	69.67	70.22	69.41	79.11	79.14	79.54	78.71	95.51	94.37	93.71	92.94
	A-Meta-Self [67]	69.79	69.95	69.08	69.48	79.11	78.25	79.02	78.44	95.51	94.71	93.33	92.75
	A-Meta-Train [67]	69.79	69.93	69.92	70.76	79.11	79.37	79.29	78.64	95.51	94.70	94.65	93.94
	GrAD [30]	69.79	70.21	70.59	70.92	79.11	79.65	79.28	78.25	95.51	<u>94.06</u>	<b>92.53</b>	<b>92.11</b>
	DGA-FOA (ours)	69.79	<u>68.88</u>	<u>67.60</u>	<u>65.48</u>	79.11	<b>77.64</b>	<u>77.22</u>	<u>75.48</u>	95.51	94.41	93.56	92.77
	DGA-FDA (ours)	69.79	<b>68.55</b>	<b>66.92</b>	<b>65.22</b>	79.11	<u>77.82</u>	<b>76.66</b>	<b>75.45</b>	95.51	94.55	94.14	92.37
	GCN-SVD [10]	DICE [53]	67.36	66.27	66.11	65.73	77.65	72.34	71.77	71.38	93.99	<u>93.19</u>	<b>91.91</b>
Meta-Self [67]		67.36	65.76	66.08	65.88	77.65	72.24	72.25	71.80	93.99	<b>93.15</b>	93.03	92.94
Meta-Train [67]		67.36	66.05	66.23	65.88	77.65	72.37	72.43	72.05	93.99	93.74	93.74	93.66
A-Meta-Self [67]		67.36	66.25	66.47	66.25	77.65	72.38	72.47	72.41	93.99	93.52	<u>92.27</u>	<b>90.75</b>
A-Meta-Train [67]		67.36	66.44	66.22	66.08	77.65	72.17	72.07	72.17	93.99	94.11	94.13	92.89
GrAD [30]		67.36	66.29	66.53	66.72	77.65	72.39	72.16	72.13	93.99	93.46	93.10	92.55
DGA-FOA (ours)		67.36	<b>65.37</b>	<u>65.01</u>	<u>65.26</u>	77.65	<u>72.10</u>	<b>71.42</b>	<b>71.26</b>	93.99	93.56	92.88	92.68
DGA-FDA (ours)		67.36	<u>65.75</u>	<b>65.98</b>	<b>65.23</b>	77.65	<b>71.85</b>	<u>71.50</u>	<u>71.35</u>	93.99	93.51	93.04	92.42
GCN-Jaccard [57]	DICE [53]	72.29	71.63	71.29	70.77	82.59	82.32	81.92	81.69	-	-	-	-
	Meta-Self [67]	72.29	71.91	<b>70.52</b>	<b>68.87</b>	82.59	81.88	<b>80.06</b>	<b>78.75</b>	-	-	-	-
	Meta-Train [67]	72.29	71.48	71.36	71.27	82.59	81.83	81.37	80.79	-	-	-	-
	A-Meta-Self [67]	72.29	71.44	71.13	70.84	82.59	82.59	81.91	81.21	-	-	-	-
	A-Meta-Train [67]	72.29	<u>71.27</u>	71.43	71.08	82.59	81.97	81.32	<u>80.46</u>	-	-	-	-
	GrAD [30]	72.29	71.60	71.33	71.34	82.59	82.33	82.11	81.57	-	-	-	-
	DGA-FOA (ours)	72.29	<b>71.24</b>	70.81	70.04	82.59	<b>81.49</b>	<u>81.02</u>	80.78	-	-	-	-
	DGA-FDA (ours)	72.29	71.41	<u>70.76</u>	<u>70.01</u>	82.59	<u>81.63</u>	81.25	80.56	-	-	-	-

**Table 5: Test accuracy (%) of the GCN model after training with clean and DGA poisoned graphs optimized with different  $k$  values in Gumbel top- $k$  trick on the Cora dataset. The best results are highlighted in bold.**

Perturbation Rate (%)	0	1	3	5
$k = 1$	83.62	80.06	78.92	78.37
$k = 2$	83.62	<b>79.89</b>	<b>78.77</b>	<b>78.07</b>
$k = 3$	83.62	79.95	<b>78.77</b>	78.32
$k = 4$	83.62	80.01	<b>78.77</b>	78.27

homophily property in social networks and citation networks and the pattern demonstrated in Waniek et al. [53].

## 6 RELATED WORK

**Adversarial Attacks on Graphs** aim to interfere with the performance of graph neural networks by introducing subtle perturbations to graph data. Following the taxonomy in recent surveys [21, 42], adversarial attacks on GNNs can be classified based on several factors, including the level of the task being performed (e.g. node-level tasks [4, 10, 54, 66] or graph-level tasks [7, 44]), the goal of the attack (e.g. targeted [57, 66] or untargeted/global attack [67]), the phase of the attack (e.g. poisoning attack [6, 28, 43]

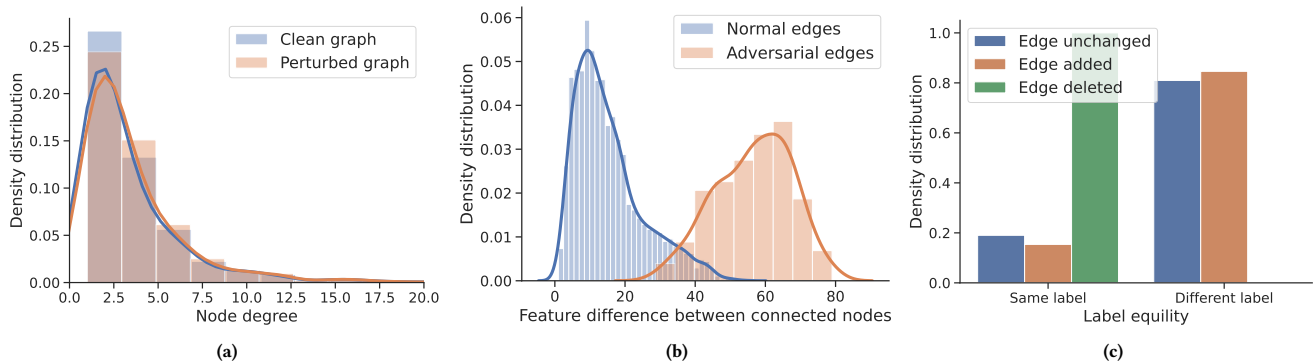


**Figure 3: Visualization of statistics of the poisoned graph compared to the original clean graph. Here we provide a comparison on (a) the node degree distribution, (b) the node feature similarity, and (c) the label equality between clean and DGA poisoned graphs on the Citeseer dataset. Note that the x-axis of the node degree distribution plot is scaled for better visualization.**

or evasion attack [4, 50]), the level of knowledge that the attacker has about the model (e.g. white-box [49, 54], black-box [7, 32, 33], or gray-box [3, 43, 67]), and the perturbation type of the attack (e.g. perturbing node features [32, 66], graph structure [29, 67], or injecting new nodes [43, 47, 65]). Different combinations of these scenarios present unique challenges and require different approaches to design effective attacks and defenses.

In this paper, we focus on a practical problem setting of *node-level, untargeted, gray-box poisoning* attack on *graph structure* [21, 29, 30, 54, 57, 67]. Previous works formulate this setting as a bi-level optimization problem and try to solve it on the discrete graph structure. MetAttack [67] first employs a meta-learning approach and treat the input data as a hyper-parameter to learn. They adopt a greedy algorithm to obtain the discrete graph structure by selecting one bit to flip at a time, iteratively for each bit in the perturbation budget. Building on the meta-learning framework, AtkSE [29] approximates the continuous distribution of hyper-gradients using discrete edge flipping intervals. GraD [30] introduced a novel attack objective to address the gradient bias. However, as illustrated in Figure 1, the meta-gradient calculation process of these approaches requires computing the Hessian matrix and accumulating trained-from-scratch inner-loop iteration, resulting in time and resource-intensive operations that are repeated until the perturbation budget is filled. To achieve effective attacks while minimizing time and resource costs, we propose a novel approach that relaxes the graph structure and learns a continuous edge probability map with attack gradients. By simultaneously updating the graph structure and surrogate model parameters, we can efficiently sample optimal perturbation sets from the learned probability map, enabling continuous budget-constrained search.

**Continuous Relaxation on Graph Structure** was first explored in graph structure learning [64]. For instance, LDS [2] incorporates a probabilistic map as a graph generator to model the adjacency matrix of the graph DGM [22] augments the graph structure using continuous updates to the graph structure with a differentiable graph module and a diffusion module. NeuralSparse [15] learns  $k$ -neighbor subgraphs for robust graph representation learning by

selecting at most  $k$  edges for each nodes. PTDNet [31] introduces a denoising map drawn from a Bernoulli distribution and learns to drop task-irrelevant edges. In contrast to these previous works, our proposed DGA, taking an adversarial learning perspective, is the first to employ continuous relaxation on graph structure and utilize learnable probabilities for attacking GNNs. Notably, Xu et al. [57] proposed a method for white-box graph attack with continuous relaxation on the perturbation map and use projected gradient descent to update the perturbations. In contrast, DGA adopts stochastic gradient descent to directly update the graph structure, enabling better flexibility, transferability and interpretability.

## 7 CONCLUSIONS, LIMITATIONS AND SOCIAL IMPACT

This paper proposes a poisoning attack model on graph-structured data. We propose a novel approach DGA, which leverages continuous relaxation and parameterization of the graph structure to generate effective and efficient attacks. DGA outperforms or approximates the state-of-the-art performance on a variety of benchmark datasets, with significantly less training time and GPU memory occupation compared to existing methods. We also provide extensive analysis of the transferability of our approach to other graph models, as well as its robustness against widely-used defense mechanisms. These can help assess the robustness of existing GNN methods, as well as guide the development of new defense strategies for adversarial attacks. Additionally, DGA can be expand to large-scale graphs simply with neighbor-sampling training mechanisms, which remains a direction for future exploration.

## ETHICAL CONSIDERATIONS

It is worth noting the potential negative social impact of this work. The proposed poisoning attack model, if misused, can significantly impact the robustness and integrity of GNNs. This is a reminder of the importance of protecting the privacy of data, including attributes of nodes, training labels, and graph structure, to prevent malicious exploitation and unauthorized attacks.



## REFERENCES

- [1] Lada A Adamic and Natalie Glance. The political blogosphere and the 2004 us election: divided they blog. In *Proceedings of the 3rd international workshop on Link discovery*, pages 36–43, 2005.
- [2] Tristan Bepler and Bonnie Berger. Learning protein sequence embeddings using information from structure. In *International Conference on Learning Representations*, 2019. URL <https://openreview.net/forum?id=SygLehCqtm>.
- [3] Aleksandar Bojchevski and Stephan Günnemann. Adversarial attacks on node embeddings via graph poisoning. In *International Conference on Machine Learning*, pages 695–704, 2019. PMLR, 2019.
- [4] Heng Chang, Yu Rong, Tingyang Xu, Wenbing Huang, Honglei Zhang, Peng Cui, Wenwu Zhu, and Junzhou Huang. A restricted black-box adversarial framework towards attacking graph embedding models. In *Proceedings of the AAAI Conference on Artificial Intelligence*, volume 34, pages 3389–3396, 2020.
- [5] Hanxiong Chen, Yunqi Li, Shaoyun Shi, Shuchang Liu, He Zhu, and Yongfeng Zhang. Graph collaborative reasoning. In *Proceedings of the Fifteenth ACM International Conference on Web Search and Data Mining*, pages 75–84, 2022.
- [6] Enyan Dai, Minhua Lin, Xiang Zhang, and Suhang Wang. Unnoticeable backdoor attacks on graph neural networks. In *Proceedings of the ACM Web Conference 2023*, pages 2263–2273, 2023.
- [7] Hanjun Dai, Hui Li, Tian Tian, Xin Huang, Lin Wang, Jun Zhu, and Le Song. Adversarial attack on graph structured data. In *International conference on machine learning*, pages 1115–1124. PMLR, 2018.
- [8] Ailin Deng and Bryan Hooi. Graph neural network-based anomaly detection in multivariate time series. In *Proceedings of the AAAI conference on artificial intelligence*, volume 35, pages 4027–4035, 2021.
- [9] Francesco Di Giovanni, Lorenzo Giusti, Federico Barbero, Giulia Luise, Pietro Lio, and Michael Bronstein. On over-squashing in message passing neural networks: The impact of width, depth, and topology. *arXiv preprint arXiv:2302.02941*, 2023.
- [10] Negin Entezari, Saba A Al-Sayouri, Amirali Darvishzadeh, and Evangelos E Papalexakis. All you need is low (rank) defending against adversarial attacks on graphs. In *Proceedings of the 13th International Conference on Web Search and Data Mining*, pages 169–177, 2020.
- [11] Wenqi Fan, Yao Ma, Qing Li, Yuan He, Eric Zhao, Jiliang Tang, and Dawei Yin. Graph neural networks for social recommendation. In *The world wide web conference*, pages 417–426, 2019.
- [12] Matthias Fey and Jan E. Lenssen. Fast graph representation learning with PyTorch Geometric. In *ICLR Workshop on Representation Learning on Graphs and Manifolds*, 2019.
- [13] Chelsea Finn, Pieter Abbeel, and Sergey Levine. Model-agnostic meta-learning for fast adaptation of deep networks. In *International conference on machine learning*, pages 1126–1135. PMLR, 2017.
- [14] Simon Geisler, Tobias Schmidt, Hakan Şirin, Daniel Zügner, Aleksandar Bojchevski, and Stephan Günnemann. Robustness of graph neural networks at scale. *Advances in Neural Information Processing Systems*, 34:7637–7649, 2021.
- [15] Justin Gilmer, Samuel S Schoenholz, Patrick F Riley, Oriol Vinyals, and George E Dahl. Neural message passing for quantum chemistry. In *Proceedings of the 34th International Conference on Machine Learning-Volume 70*, pages 1263–1272. JMLR.org, 2017.
- [16] Ian Goodfellow, Jonathon Shlens, and Christian Szegedy. Explaining and harnessing adversarial examples. In *International Conference on Learning Representations*, 2015. URL <http://arxiv.org/abs/1412.6572>.
- [17] Will Hamilton, Zitao Ying, and Jure Leskovec. Inductive representation learning on large graphs. *Advances in neural information processing systems*, 30, 2017.
- [18] Yue Hu, Ao Qu, and Dan Work. Detecting extreme traffic events via a context augmented graph autoencoder. *ACM Transactions on Intelligent Systems and Technology (TIST)*, 13(6):1–23, 2022.
- [19] John Ingraham, Vikas Garg, Regina Barzilay, and Tommi Jaakkola. Generative models for graph-based protein design. *Advances in Neural Information Processing Systems*, 32, 2019.
- [20] Wei Jin, Yao Ma, Xiaorui Liu, Xianfeng Tang, Suhang Wang, and Jiliang Tang. Graph structure learning for robust graph neural networks. In *Proceedings of the 26th ACM SIGKDD international conference on knowledge discovery & data mining*, pages 66–74, 2020.
- [21] Wei Jin, Yaxing Li, Han Xu, Yiqi Wang, Shuiwang Ji, Charu Aggarwal, and Jiliang Tang. Adversarial attacks and defenses on graphs. *ACM SIGKDD Explorations Newsletter*, 22(2):19–34, 2021.
- [22] Anees Kazi, Luca Cosmo, Seyed-Ahmad Ahmadi, Nassir Navab, and Michael M Bronstein. Differentiable graph module (dgm) for graph convolutional networks. *IEEE Transactions on Pattern Analysis and Machine Intelligence*, 45(2):1606–1617, 2022.
- [23] Diederik P Kingma and Jimmy Ba. Adam: A method for stochastic optimization. *International Conference on Learning Representation*, 2014.
- [24] Thomas N. Kipf and Max Welling. Semi-supervised classification with graph convolutional networks. In *International Conference on Learning Representations*, 2017. URL <https://openreview.net/forum?id=SJU4ayYgl>.
- [25] Wouter Kool, Herke Van Hoof, and Max Welling. Stochastic beams and where to find them: The gumbel-top-k trick for sampling sequences without replacement. In *International Conference on Machine Learning*, pages 3499–3508. PMLR, 2019.
- [26] Yaxin Li, Wei Jin, Han Xu, and Jiliang Tang. Deeprobust: A pytorch library for adversarial attacks and defenses. *arXiv preprint arXiv:2005.06149*, 2020.
- [27] Hanxiao Liu, Karen Simonyan, and Yiming Yang. DARTS: Differentiable architecture search. In *International Conference on Learning Representations*, 2019. URL <https://openreview.net/forum?id=S1eYHoC5FX>.
- [28] Xuanqing Liu, Si Si, Xiaojin Zhu, Yang Li, and Cho-Jui Hsieh. A unified framework for data poisoning attack to graph-based semi-supervised learning. In *Proceedings of the 33rd International Conference on Neural Information Processing Systems*, pages 9780–9790, 2019.
- [29] Zihan Liu, Yun Luo, Lirong Wu, Siyuan Li, Zicheng Liu, and Stan Z Li. Are gradients on graph structure reliable in gray-box attacks? In *Proceedings of the 31st ACM International Conference on Information & Knowledge Management*, pages 1360–1368, 2022.
- [30] Zihan Liu, Yun Luo, Lirong Wu, Zicheng Liu, and Stan Z. Li. Towards reasonable budget allocation in untargeted graph structure attacks via gradient debias. In Alice H. Oh, Alekh Agarwal, Danielle Belgrave, and Kyunghyun Cho, editors, *Advances in Neural Information Processing Systems*, 2022. URL <https://openreview.net/forum?id=vkGk2HI8oOP>.
- [31] Dongsheng Luo, Wei Cheng, Wenchao Yu, Bo Zong, Jingchao Ni, Haifeng Chen, and Xiang Zhang. Learning to drop: Robust graph neural network via topological denoising. In *Proceedings of the 14th ACM international conference on web search and data mining*, pages 779–787, 2021.
- [32] Jiaqi Ma, Shuangrui Ding, and Qiaozhu Mei. Towards more practical adversarial attacks on graph neural networks. *Advances in neural information processing systems*, 33:4756–4766, 2020.
- [33] Jiaqi Ma, Junwei Deng, and Qiaozhu Mei. Adversarial attack on graph neural networks as an influence maximization problem. In *Proceedings of the Fifteenth ACM International Conference on Web Search and Data Mining*, pages 675–685, 2022.
- [34] Aleksander Madry, Aleksandar Makelov, Ludwig Schmidt, Dimitris Tsipras, and Adrian Vladu. Towards deep learning models resistant to adversarial attacks. In *International Conference on Learning Representations*, 2018. URL <https://openreview.net/forum?id=rjZiBzAb>.
- [35] Andrew Kachites McCallum, Kamal Nigam, Jason Rennie, and Kristie Seymore. Automating the construction of internet portals with machine learning. *Information Retrieval*, 3:127–163, 2000.
- [36] Yitong Pang, Lingfei Wu, Qi Shen, Yiming Zhang, Zhihua Wei, Fangli Xu, Ethan Chang, Bo Long, and Jian Pei. Heterogeneous global graph neural networks for personalized session-based recommendation. In *Proceedings of the fifteenth ACM international conference on web search and data mining*, pages 775–783, 2022.
- [37] Adam Paszke, Sam Gross, Francisco Massa, Adam Lerer, James Bradbury, Gregory Chanan, Trevor Killeen, Zeming Lin, Natalia Gimelshein, Luca Antiga, et al. PyTorch: An imperative style, high-performance deep learning library. *Advances in neural information processing systems*, 32, 2019.
- [38] Bryan Perozzi, Rami Al-Rfou, and Steven Skiena. Deepwalk: Online learning of social representations. In *Proceedings of the 20th ACM SIGKDD international conference on Knowledge discovery and data mining*, pages 701–710, 2014.
- [39] Benedek Rozemberczki, Carl Allen, and Rik Sarkar. Multi-scale attributed node embedding. *Journal of Complex Networks*, 9(2):enab014, 2021.
- [40] Prithviraj Sen, Galileo Namata, Mustafa Bilgic, Lise Getoor, Brian Galligher, and Tina Eliassi-Rad. Collective classification in network data. *AI magazine*, 29(3): 93–93, 2008.
- [41] Hannes Stärk, Octavian Ganea, Lagnajit Pattanaik, Regina Barzilay, and Tommi Jaakkola. EquiBind: Geometric deep learning for drug binding structure prediction. In *International Conference on Machine Learning*, pages 20503–20521. PMLR, 2022.
- [42] Lichao Sun, Yingdong Dou, Carl Yang, Kai Zhang, Ji Wang, S Yu Philip, Lifang He, and Bo Li. Adversarial attack and defense on graph data: A survey. *IEEE Transactions on Knowledge and Data Engineering*, 2022.
- [43] Yiwei Sun, Suhang Wang, Xianfeng Tang, Tsung-Yu Hsieh, and Vasant Honavar. Adversarial attacks on graph neural networks via node injections: A hierarchical reinforcement learning approach. In *Proceedings of The Web Conference 2020*, WWW '20, page 673–683, New York, NY, USA, 2020. Association for Computing Machinery. ISBN 9781450370233. doi: 10.1145/3366423.3380149. URL <https://doi.org/10.1145/3366423.3380149>.
- [44] Haoteng Tang, Guixiang Ma, Yurong Chen, Lei Guo, Wei Wang, Bo Zeng, and Liang Zhan. Adversarial attack on hierarchical graph pooling neural networks. *arXiv preprint arXiv:2005.11560*, 2020.
- [45] Xianfeng Tang, Yandong Li, Yiwei Sun, Huaxiu Yao, Prasenjit Mitra, and Suhang Wang. Transferring robustness for graph neural network against poisoning attacks. In *Proceedings of the 13th international conference on web search and data mining*, pages 600–608, 2020.
- [46] Xianfeng Tang, Yozen Liu, Xinran He, Suhang Wang, and Neil Shah. Friend story ranking with edge-contextual local graph convolutions. In *Proceedings of the Fifteenth ACM International Conference on Web Search and Data Mining*, pages

- 1007–1015, 2022.
- [47] Shuchang Tao, Huawei Shen, Qi Cao, Liang Hou, and Xueqi Cheng. Adversarial immunization for certifiable robustness on graphs. In *Proceedings of the 14th ACM International Conference on Web Search and Data Mining*, pages 698–706, 2021.
- [48] Petar Veličković, Guillem Cucurull, Arantxa Casanova, Adriana Romero, Pietro Liò, and Yoshua Bengio. Graph attention networks. In *International Conference on Learning Representations*, 2018. URL <https://openreview.net/forum?id=rjXmpikCZ>.
- [49] Binghui Wang and Neil Zhenqiang Gong. Attacking graph-based classification via manipulating the graph structure. In *Proceedings of the 2019 ACM SIGSAC Conference on Computer and Communications Security*, pages 2023–2040, 2019.
- [50] Binghui Wang, Tianxiang Zhou, Minhua Lin, Pan Zhou, Ang Li, Meng Pang, Cai Fu, Hai Li, and Yiran Chen. Evasion attacks to graph neural networks via influence function. *arXiv preprint arXiv:2009.00203*, 2020.
- [51] Binghui Wang, Jinyuan Jia, Xiaoyu Cao, and Neil Zhenqiang Gong. Certified robustness of graph neural networks against adversarial structural perturbation. In *Proceedings of the 27th ACM SIGKDD Conference on Knowledge Discovery & Data Mining*, KDD '21, page 1645–1653, New York, NY, USA, 2021. Association for Computing Machinery. ISBN 9781450383325. doi: 10.1145/3447548.3467295. URL <https://doi.org/10.1145/3447548.3467295>.
- [52] Shoujin Wang, Liang Hu, Yan Wang, Xiangnan He, Quan Z Sheng, Mehmet A Orgun, Longbing Cao, Francesco Ricci, and S Yu Philip. Graph learning based recommender systems: a review. In *30th International Joint Conference on Artificial Intelligence, IJCAI 2021*, pages 4644–4652. International Joint Conferences on Artificial Intelligence, 2021.
- [53] Marcin Waniek, Tomasz P Michalak, Michael J Wooldridge, and Talal Rahwan. Hiding individuals and communities in a social network. *Nature Human Behaviour*, 2(2):139–147, 2018.
- [54] Huijun Wu, Chen Wang, Yuriy Tyshetskiy, Andrew Docherty, Kai Lu, and Liming Zhu. Adversarial examples for graph data: deep insights into attack and defense. In *Proceedings of the 28th International Joint Conference on Artificial Intelligence*, pages 4816–4823, 2019.
- [55] Sang Michael Xie and Stefano Ermon. Reparameterizable subset sampling via continuous relaxations. In *International Joint Conference on Artificial Intelligence*, 2019.
- [56] Han Xu, Yaxin Li, Wei Jin, and Jiliang Tang. Adversarial attacks and defenses: Frontiers, advances and practice. In *Proceedings of the 26th ACM SIGKDD International Conference on Knowledge Discovery & Data Mining*, pages 3541–3542, 2020.
- [57] Kaidi Xu, Hongge Chen, Sijia Liu, Pin-Yu Chen, Tsui Wei Weng, Mingyi Hong, and Xue Lin. Topology attack and defense for graph neural networks: An optimization perspective. In *International Joint Conference on Artificial Intelligence*. International Joint Conferences on Artificial Intelligence, 2019.
- [58] Rex Ying, Ruining He, Kaifeng Chen, Pong Eksombatchai, William L Hamilton, and Jure Leskovec. Graph convolutional neural networks for web-scale recommender systems. In *Proceedings of the 24th ACM SIGKDD international conference on knowledge discovery & data mining*, pages 974–983, 2018.
- [59] Mengmei Zhang, Xiao Wang, Meiqi Zhu, Chuan Shi, Zhiqiang Zhang, and Jun Zhou. Robust heterogeneous graph neural networks against adversarial attacks. In *Proceedings of the AAAI Conference on Artificial Intelligence*, volume 36, pages 4363–4370, 2022.
- [60] Xiang Zhang and Marinka Zitnik. Gnn-guard: Defending graph neural networks against adversarial attacks. In *Proceedings of Neural Information Processing Systems, NeurIPS*, 2020.
- [61] Kai Zhao, Yukun Zheng, Tao Zhuang, Xiang Li, and Xiaoyi Zeng. Joint learning of e-commerce search and recommendation with a unified graph neural network. In *Proceedings of the Fifteenth ACM International Conference on Web Search and Data Mining*, pages 1461–1469, 2022.
- [62] Lingxiao Zhao and Leman Akoglu. Pairnorm: Tackling oversmoothing in gnns. In *International Conference on Learning Representations*, 2020. URL <https://openreview.net/forum?id=rkecl1rtwB>.
- [63] Qi Zhu, Natalia Ponomareva, Jiawei Han, and Bryan Perozzi. Shift-robust gnns: Overcoming the limitations of localized graph training data. *Advances in Neural Information Processing Systems*, 34:27965–27977, 2021.
- [64] Yanqiao Zhu, Weizhi Xu, Jinghao Zhang, Yuanqi Du, Jieyu Zhang, Qiang Liu, Carl Yang, and Shu Wu. A survey on graph structure learning: Progress and opportunities. *arXiv e-prints*, pages arXiv–2103, 2021.
- [65] Xu Zou, Qinkai Zheng, Yuxiao Dong, Xinyu Guan, Evgeny Kharlamov, Jialiang Lu, and Jie Tang. Tdgia: Effective injection attacks on graph neural networks. In *Proceedings of the 27th ACM SIGKDD Conference on Knowledge Discovery & Data Mining*, pages 2461–2471, 2021.
- [66] Daniel Zügner, Amir Akbarnejad, and Stephan Günnemann. Adversarial attacks on neural networks for graph data. In *Proceedings of the 24th ACM SIGKDD international conference on knowledge discovery & data mining*, pages 2847–2856, 2018.
- [67] Daniel Zügner and Stephan Günnemann. Adversarial attacks on graph neural networks via meta learning. In *International Conference on Learning Representations*, 2019. URL <https://openreview.net/forum?id=Bylnx209YX>.

## A PROOF OF THEOREM 2

First, we formally state the assumptions of Theorem 2.

**Assumption 2.** For any  $\theta, \theta' \in \mathbb{R}^D, \mathbf{q}, \mathbf{q}' \in \mathbb{R}^{N^2}$ , there exist  $G_1, G_2, L_{1,2}, L_{2,1}, L_{2,2}, H_{1,2} > 0$  such that

$$\begin{aligned} \|\mathcal{L}_{atk}(\theta, \mathbf{q}) - \mathcal{L}_{atk}(\theta', \mathbf{q})\|_2 &\leq G_1 \|\theta - \theta'\|_2, \\ \max \{ \|\mathcal{L}_{atk}(\theta, \mathbf{q}) - \mathcal{L}_{atk}(\theta, \mathbf{q}')\|_2, \\ \|\mathcal{L}_{train}(\theta, \mathbf{q}) - \mathcal{L}_{train}(\theta, \mathbf{q}')\|_2 \} &\leq G_2 \|\mathbf{q} - \mathbf{q}'\|_2, \\ \|\nabla_2 \mathcal{L}_{atk}(\theta, \mathbf{q}) - \nabla_2 \mathcal{L}_{atk}(\theta', \mathbf{q})\|_2 &\leq L_{2,1} \|\theta - \theta'\|_2, \\ \|\nabla_2 \mathcal{L}_{atk}(\theta, \mathbf{q}) - \nabla_2 \mathcal{L}_{atk}(\theta, \mathbf{q}')\|_2 &\leq L_{2,2} \|\mathbf{q} - \mathbf{q}'\|_2, \\ \|\nabla_1 \mathcal{L}_{train}(\theta, \mathbf{q}) - \nabla_1 \mathcal{L}_{train}(\theta, \mathbf{q}')\|_2 &\leq L_{1,2} \|\mathbf{q} - \mathbf{q}'\|_2, \\ \|\nabla_{1,2}^2 \mathcal{L}_{train}(\theta, \mathbf{q}) - \nabla_{1,2}^2 \mathcal{L}_{train}(\theta, \mathbf{q}')\|_F &\leq H_{1,2} \|\mathbf{q} - \mathbf{q}'\|_2, \end{aligned}$$

where  $\|\cdot\|_F$  refers to the Frobenius norm.

**Lemma 3.** Under Assumption 2, there exists  $G > 0$  and  $L > 0$  such that  $\Phi$  is  $G$ -Lipschitz continuous and  $\nabla\Phi$  is  $L$ -Lipschitz continuous.

**PROOF.** Note that  $\nabla\Phi(\mathbf{q}) = \nabla_2 \mathcal{L}_{atk}(\hat{\theta}, \mathbf{q}) - \alpha \nabla_{1,2}^2 \mathcal{L}_{train}(\theta, \mathbf{q}) \nabla_1 \mathcal{L}_{atk}(\hat{\theta}, \mathbf{q})$ .

First, we can obtain that

$$\|\nabla\Phi(\mathbf{q})\| \leq G_2 + \sqrt{\min(D, N^2)} \alpha L_{1,2} G_1.$$

For any  $\mathbf{q}, \mathbf{q}'$ , we define that  $\hat{\theta}' = \theta - \alpha \nabla_{\theta} \mathcal{L}_{train}(\theta, \mathbf{q}')$  such that

$$\begin{aligned} \|\nabla\Phi(\mathbf{q}) - \nabla\Phi(\mathbf{q}')\|_2 &\leq \|\nabla_2 \mathcal{L}_{atk}(\hat{\theta}, \mathbf{q}) - \nabla_2 \mathcal{L}_{atk}(\hat{\theta}', \mathbf{q}')\|_2 \\ &\quad + \alpha \|\nabla_{1,2}^2 \mathcal{L}_{train}(\theta, \mathbf{q}) \nabla_1 \mathcal{L}_{atk}(\hat{\theta}, \mathbf{q}) \\ &\quad - \nabla_{1,2}^2 \mathcal{L}_{train}(\theta, \mathbf{q}') \nabla_1 \mathcal{L}_{atk}(\hat{\theta}', \mathbf{q}')\|_2 \\ &\leq \|\nabla_2 \mathcal{L}_{atk}(\hat{\theta}, \mathbf{q}) - \nabla_2 \mathcal{L}_{atk}(\hat{\theta}', \mathbf{q}')\|_2 \\ &\quad + \alpha \|\nabla_{1,2}^2 \mathcal{L}_{train}(\theta, \mathbf{q})\|_F \|\nabla_1 \mathcal{L}_{atk}(\hat{\theta}, \mathbf{q}) - \nabla_1 \mathcal{L}_{atk}(\hat{\theta}', \mathbf{q}')\|_2 \\ &\quad + \alpha \|\nabla_{1,2}^2 \mathcal{L}_{train}(\theta, \mathbf{q}) - \nabla_{1,2}^2 \mathcal{L}_{train}(\theta, \mathbf{q}')\|_F \|\nabla_1 \mathcal{L}_{atk}(\hat{\theta}', \mathbf{q}')\|_2 \\ &\leq (1 + \alpha \sqrt{\min(D, N^2)} L_{1,2}) \|\nabla_2 \mathcal{L}_{atk}(\hat{\theta}, \mathbf{q}) \\ &\quad - \nabla_2 \mathcal{L}_{atk}(\hat{\theta}', \mathbf{q}')\|_2 + \alpha G_1 H_{1,2} \|\mathbf{q} - \mathbf{q}'\|_2. \end{aligned}$$

We further have

$$\begin{aligned} &\|\nabla_2 \mathcal{L}_{atk}(\hat{\theta}, \mathbf{q}) - \nabla_2 \mathcal{L}_{atk}(\hat{\theta}', \mathbf{q}')\|_2 \\ &\leq \|\nabla_2 \mathcal{L}_{atk}(\hat{\theta}, \mathbf{q}) - \nabla_2 \mathcal{L}_{atk}(\hat{\theta}, \mathbf{q}')\|_2 \\ &\quad + \|\nabla_2 \mathcal{L}_{atk}(\hat{\theta}, \mathbf{q}') - \nabla_2 \mathcal{L}_{atk}(\hat{\theta}', \mathbf{q}')\|_2 \\ &\leq L_{2,2} \|\mathbf{q} - \mathbf{q}'\|_2 + L_{2,1} \|\hat{\theta} - \hat{\theta}'\|_2 \\ &= L_{2,2} \|\mathbf{q} - \mathbf{q}'\|_2 + \alpha L_{2,1} \|\nabla_{\theta} \mathcal{L}_{train}(\theta, \mathbf{q}) \\ &\quad - \nabla_{\theta} \mathcal{L}_{train}(\theta, \mathbf{q}')\|_2 \leq (L_{2,2} + \alpha L_{1,2} L_{2,1}) \|\mathbf{q} - \mathbf{q}'\|_2 \end{aligned}$$

We define  $G := G_2 + \alpha \sqrt{\min(D, N^2)} L_{1,2} G_1$  and  $L := (1 + \alpha \sqrt{\min(D, N^2)} L_{1,2}) (L_{2,2} + \alpha L_{1,2} L_{2,1}) + \alpha G_1 H_{1,2}$ .  $\square$

**PROOF OF THEOREM 2.** By the  $L$ -Lipschitzness of  $\nabla\Phi$  as shown Lemma 3, we have

$$\begin{aligned} \mathbb{E}_t \Phi(\mathbf{q}_{t+1}) &\leq \Phi(\mathbf{q}_t) - \eta \nabla\Phi(\mathbf{q}_t) \cdot \mathbb{E}_t \nabla\Phi(\tilde{\mathbf{q}}_t) \\ &\quad + \eta^2 L \mathbb{E}_t \|\nabla\Phi(\tilde{\mathbf{q}}_t) - \nabla\Phi(\mathbf{q}_t)\|_2^2 + \eta^2 L \|\Phi(\mathbf{q}_t)\|_2^2 \\ &\leq \Phi(\mathbf{q}_t) - \eta \nabla\Phi(\mathbf{q}_t) \cdot \mathbb{E}_t \nabla\Phi(\tilde{\mathbf{q}}_t) \\ &\quad + \eta^2 L^3 \mathbb{E}_t \|\tilde{\mathbf{q}}_t - \mathbf{q}_t\|_2^2 + \eta^2 L \|\Phi(\mathbf{q}_t)\|_2^2, \end{aligned} \quad (7)$$

where  $\mathbb{E}_t[\cdot]$  refers to the expectation conditioned on the randomness before iteration  $t$ . Young's inequalities leads to

$$\begin{aligned} &-\eta \nabla\Phi(\mathbf{q}_t) \cdot \mathbb{E}_t \nabla\Phi(\tilde{\mathbf{q}}_t) \\ &= -\eta \|\nabla\Phi(\mathbf{q}_t)\|_2^2 - \eta \mathbb{E}_t [\nabla\Phi(\mathbf{q}_t) \cdot (\nabla\Phi(\tilde{\mathbf{q}}_t) - \nabla\Phi(\mathbf{q}_t))] \\ &\leq -\frac{\eta}{2} \|\nabla\Phi(\mathbf{q}_t)\|_2^2 + \frac{\eta}{2} \mathbb{E}_t [\|\nabla\Phi(\tilde{\mathbf{q}}_t) - \nabla\Phi(\mathbf{q}_t)\|_2^2] \\ &\leq -\frac{\eta}{2} \|\nabla\Phi(\mathbf{q}_t)\|_2^2 + \frac{\eta L^2}{2} \mathbb{E}_t [\|\tilde{\mathbf{q}}_t - \mathbf{q}_t\|_2^2]. \end{aligned} \quad (8)$$

Plug (8) into (7) and re-arrange the terms.

$$\begin{aligned} &\mathbb{E}_t \Phi(\mathbf{q}_{t+1}) \\ &\leq \Phi(\mathbf{q}_t) - \frac{\eta}{2} (1 - 2\eta L) \|\nabla\Phi(\mathbf{q}_t)\|_2^2 + \frac{\eta L^2}{2} (1 + 2\eta L) \mathbb{E}_t \|\tilde{\mathbf{q}}_t - \mathbf{q}_t\|_2^2. \end{aligned}$$

Set  $\eta = \frac{1}{4L}$  and use the tower property of expectation.

$$\mathbb{E} \|\nabla\Phi(\mathbf{q}_t)\|_2^2 \leq 16L \mathbb{E} [\Phi(\mathbf{q}_t) - \Phi(\mathbf{q}_{t+1})] + 3L^2 \mathbb{E} \|\tilde{\mathbf{q}}_t - \mathbf{q}_t\|_2^2.$$

Do telescoping sum from  $t = 0$  to  $T - 1$  and divide  $T$  on both sides.

$$\frac{1}{T} \sum_{t=0}^{T-1} \mathbb{E} \|\nabla\Phi(\mathbf{q}_t)\|_2^2 \leq \frac{16L(\Phi(\mathbf{q}_0) - \inf_{\mathbf{q}} \Phi)}{T} + \frac{3L^2}{T} \sum_{t=0}^{T-1} \mathbb{E} \|\tilde{\mathbf{q}}_t - \mathbf{q}_t\|_2^2. \quad \square$$

## B EXPERIMENTAL SETUP

### B.1 Dataset Description

**CiteSeer** [40] is a citation network containing 3,312 scientific publications classified into 6 classes. The network consists of 4,732 links, and each publication is represented by a binary word vector indicating the presence or absence of words from a dictionary of 3,703 unique words.

**Cora** [35] is another citation network comprising 2,708 scientific publications classified into seven classes. The network includes 5,429 links, and each publication is represented by a binary word vector indicating the presence or absence of words from a dictionary of 1,433 unique words.

**PolBlogs** [1] is a graph with 1,490 vertices representing political blogs and 19,025 edges representing links between blogs. The links are automatically extracted from the front pages of blogs. Each vertex is labeled as either liberal or conservative, indicating the political leaning of the blog.

### B.2 Implementation Details.

Our method is implemented using PyTorch [37] and PyTorch Geometric [12] frameworks, with training conducted using the Adam optimizer [23]. The experiments are carried out on a single NVIDIA RTX A5000 24GB GPU. The search space for model and training hyperparameters can be found in Table 6. Note that the number of finetuning iterations is applicable to DGA-FOA only, whereas for

DGA-FDA, it is set to 1, indicating one-step optimization. For all experiments, optimal hyperparameters are selected based on the performance of the validation set.

### B.3 Base Model Description

**Graph Attention Network (GAT)** [48] is a neural network architecture that performs graph convolutions using attention mechanisms to selectively aggregate information from neighboring nodes. It is frequently employed as a foundational layer of defense against adversarial attacks.

**DeepWalk** [38] is an unsupervised learning method that aims to learn low-dimensional representations of nodes in a graph. It generates random walks within the graph and applies the skip-gram model to learn node embeddings. As DeepWalk is trained in an unsupervised manner without node characteristics or graph convolutions, this transfer setting is more challenging.

**GCN-Jaccard** [54] is a defense method that focuses on identifying and removing adversarial nodes in a graph. The Jaccard similarity between the neighborhood sets of two nodes is used to determine if a node is likely to be adversarial. By identifying and removing such nodes, GCN-Jaccard aims to improve the robustness of graph models against adversarial attacks.

**GCN-SVD** [10] is a defense method that mitigates adversarial attacks by approximating the graph Laplacian with a low-rank matrix. By reducing the dimensionality of the graph Laplacian, GCN-SVD aims to preserve the essential structural information while suppressing the influence of potential adversarial perturbations.

### B.4 Baseline Reproduction Detail

**DICE** [53] (Delete Internally, Connect Externally) is an attack method that focuses on modifying the graph structure to undermine the performance of targeted models. It achieves this by randomly connecting nodes with different labels or removing edges between nodes with the same label. This manipulation of the graph aims to disrupt the original connectivity patterns and induce misclassification errors in the targeted model. For our implementation of the DICE attack, we use the code provided in the DeepRobust package [26].

**MetAttack** [67] is an attack method that utilizes meta-learning to solve a bi-level optimization problem. It employs a greedy approach to selectively perturb one edge at a time in order to maximize the adversarial impact on the targeted model. The method includes four variants of MetAttack, each employing different loss functions and incorporating first-order approximation: Meta-Train, Meta-Self, A-Meta-Train, and A-Meta-Self. Note that the “Train” variants use cross-entropy loss on the training set, while the “Self” variants use self-training loss with pseudo labels. The “A-” variants indicate the use of first-order approximations during the optimization process. For reproduction, we rely on the code available in the DeepRobust package [26] with the default hyperparameters included with the code.

**GraD** [30] is a recent attack method that leverages the meta-learning framework and introduces a novel attack objective to mitigate gradient bias. It claims that it outperforms MetAttack in terms of overall graph performance across the datasets, rather than only focusing on the largest connected component. For reproduction,

we use the official code and the default hyperparameters provided at <https://github.com/Zihan-Liu-00/GraD--NeurIPS22>.

## C ADDITIONAL EXPERIMENTAL RESULTS

### C.1 Results with standard deviation

The standard deviations of the experiments conducted on the GCN, GAT, DeepWalk, and GCN model vaccinated with low-rank SVD approximation (GCN-SVD), and Jaccard (GCN-Jaccard) methods, as described in Section 5, are presented in Tables 7 to 11, respectively. The standard deviations are calculated based on 10 runs, providing a reliable estimation of the variation in the experimental results. This indicates that our method consistently performs well and exhibits relatively low variability, thereby highlighting its effectiveness and reliability. These results demonstrate the robustness and stability of our proposed method.

### C.2 Computation Complexity with 1% and 3% Perturbation Rates

Table 12 and Table 13 provide a comparison of training time and peak GPU memory usage between the proposed DGA method and the baselines, considering perturbation rates of 1% and 3% respectively. Our approach demonstrates notable advantages over baselines, including significantly reduced training time and lower memory usage. Importantly, our method maintains consistent computational efficiency even as the perturbation rate increases. These results highlight the computational benefits of DGA, making it an efficient and scalable solution for adversarial attacks on graph structures. Furthermore, the substantial reductions in training time and GPU memory usage also imply the promising potential of DGA for real-world applications, particularly when dealing with large-scale graphs.

### C.3 Visualization for Cora and Polblogs Datasets

We present a visual comparison of statistics between the poisoned graph generated by DGA and the original clean graph. Specifically, we analyze the node degree distribution, node feature similarity, and label equality on the Cora and Polblogs datasets, as shown in Figure 4. To enhance clarity and improve visualization, we scale the x-axis of the node degree distribution plot. Notably, we consistently observe similar trends and patterns in these statistics across the Cora and Polblogs datasets, reaffirming our previous observations on the Citeseer dataset as outlined in Sec. 5.2. By conducting a visual comparison of these statistics, we gain a better understanding of the attack’s influence on the graph structure and its implications for the performance and behavior of the targeted model. This analysis significantly contributes to our comprehensive evaluation and assessment of the effectiveness and impacts of the proposed DGA method.

Received 20 February 2007; revised 12 March 2009; accepted 5 June 2009

**Table 6: Model and training hyperparameters for our method on different tasks.**

Hyperparameter	Values/Search Space		
	CiteSeer	Cora	PolBlogs
Momentum	0.9	0.9	0.9
#Iters of attack	100, 150, 200, 500	100, 150, 200	100, 150, 200, 500
Attack step size $\eta$	1e-2, 5e-3, 1e-3, 5e-4, 1e-4, 5e-5, 1e-5	1e-2, 5e-3, 1e-3, 5e-4, 1e-4	1e-2, 5e-3, 1e-3, 5e-4, 1e-4
#Iters of finetuning (DGA-FOA)	50, 100, 150, 200	50, 100, 150, 200	50, 100, 150, 200
Finetune step size $\alpha$	1e-2, 5e-3, 1e-3, 5e-4, 1e-4, 5e-5, 1e-5	1e-2, 5e-3, 1e-3, 5e-4, 1e-4	1e-2, 5e-3, 1e-3, 5e-4, 1e-4
Gumbel $\tau$	1.0	1.0	1.0
Gumbel $k$	1,2,3,4,5	2,3,4,5,6	5, 10, 15, 20, 25

**Table 7: Standard deviations of test accuracies (%) for GCN models trained on both clean and poisoned graphs.**

Dataset	CiteSeer				Cora				PolBlogs			
	Perturbation Rate (%)	0	1	3	5	0	1	3	5	0	1	3
DICE [53]	0.6	0.67	0.60	0.81	1.16	0.98	0.99	1.13	0.42	0.42	0.40	0.67
Meta-Self [67]	0.6	0.87	1.30	1.91	1.16	2.12	2.28	2.29	0.42	0.53	0.98	0.41
Meta-Train [67]	0.6	1.23	0.8	0.78	1.16	1.21	1.26	1.47	0.42	0.53	1.53	1.38
A-Meta-Self [67]	0.6	0.85	1.20	1.29	1.16	1.08	1.37	1.25	0.42	0.66	0.7	0.83
A-Meta-Train [67]	0.6	0.68	1.06	1.31	1.16	1.08	1.22	1.25	0.42	0.59	2.66	2.72
GraD [30]	0.6	0.66	0.63	1.02	1.16	0.96	1.22	0.92	0.42	1.08	1.46	1.41
DGA-FOA (ours)	0.6	0.49	0.56	0.61	1.16	1.22	1.1	1.1	0.42	0.6	0.88	0.91
DGA-FDA (ours)	0.6	0.88	0.82	0.75	1.16	1.14	1.16	1.16	0.42	0.84	0.78	0.92

**Table 8: Standard deviations of test accuracies (%) for GAT models after training with clean and poisoned graphs.**

Dataset	CiteSeer				Cora				PolBlogs			
	Perturbation Rate (%)	0	1	3	5	0	1	3	5	0	1	3
DICE [53]	1.00	0.53	0.96	0.94	0.84	0.76	0.99	0.9	0.51	0.62	0.73	0.49
Meta-Self [67]	1.00	0.8	0.8	1.12	0.84	1.1	0.86	0.56	0.51	0.56	0.67	0.88
Meta-Train [67]	1.00	1.36	0.72	1.21	0.84	0.94	0.84	1.07	0.51	0.67	1.15	1.27
A-Meta-Self [67]	1.00	1.37	1.05	0.89	0.84	0.95	1.21	0.76	0.51	0.61	1.02	1.14
A-Meta-Train [67]	1.00	0.89	1.13	1.08	0.84	0.97	0.81	0.84	0.51	0.74	0.86	0.62
GraD [30]	1.00	1.17	0.82	1.11	0.84	0.7	1.04	0.79	0.51	0.49	0.66	0.54
DGA-FOA (ours)	1.00	0.4	0.85	0.94	0.84	0.87	1.07	0.64	0.51	0.82	0.55	0.37
DGA-FDA (ours)	1.00	0.87	1.08	1.09	0.84	0.7	0.47	0.64	0.51	0.53	0.58	0.65

**Table 9: Standard deviations of test accuracies (%) for DeepWalk models after training with clean and poisoned graphs.**

Dataset	CiteSeer				Cora				PolBlogs			
	Perturbation Rate (%)	0	1	3	5	0	1	3	5	0	1	3
Meta-Self [67]	0.95	1.03	1.57	0.9	0.97	0.62	0.79	0.7	0.42	0.5	0.52	0.93
Meta-Train [67]	0.95	1.0	0.67	1.71	0.97	0.9	0.63	0.93	0.42	0.65	0.65	0.79
A-Meta-Self [67]	0.95	0.94	1.5	0.98	0.97	0.67	0.8	0.58	0.42	0.54	0.51	0.59
A-Meta-Train [67]	0.95	0.83	0.88	1.27	0.97	0.86	0.93	0.73	0.42	0.65	0.58	0.57
GraD [30]	0.95	0.49	0.9	1.31	0.97	0.49	0.53	0.85	0.42	0.74	0.53	0.69
DGA-FOA (ours)	0.95	1.11	0.55	0.97	0.97	0.83	0.8	1.07	0.42	0.29	0.49	0.39
DGA-FDA (ours)	0.95	1.24	0.91	1.11	0.97	0.87	1.0	1.13	0.42	0.43	0.69	0.54

**Table 10: Standard deviations of test accuracies (%) for the GCN model vaccinated with low-rank SVD approximation.**

Dataset Perturbation Rate (%)	CiteSeer				Cora				PolBlogs			
	0	1	3	5	0	1	3	5	0	1	3	5
DICE [53]	1.40	1.35	1.51	1.84	1.04	0.72	0.97	0.92	0.42	0.5	0.65	0.61
Meta-Self [67]	1.40	1.6	1.64	1.15	1.04	0.79	0.78	0.64	0.42	0.82	0.94	0.89
Meta-Train [67]	1.40	1.49	1.64	2.09	1.04	0.57	0.92	0.6	0.42	0.62	0.58	0.44
A-Meta-Self [67]	1.40	1.31	1.01	1.34	1.04	0.61	0.68	0.81	0.42	0.59	0.73	1.04
A-Meta-Train [67]	1.40	1.41	1.18	1.75	1.04	0.72	0.77	0.83	0.42	0.53	0.57	1.09
GraD [30]	1.40	1.3	1.28	1.11	1.04	0.62	0.72	0.82	0.42	0.61	0.57	0.78
DGA-FOA (ours)	1.40	1.34	1.53	1.54	1.04	0.45	0.72	0.52	0.42	0.61	0.6	0.75
DGA-FDA (ours)	1.40	0.91	1.53	1.52	1.04	0.66	0.54	0.73	0.42	0.53	0.44	0.62

**Table 11: Test accuracy (%) of the GCN model vaccinated with Jaccard.**

Dataset Perturbation Rate (%)	CiteSeer				Cora			
	0	1	3	5	0	1	3	5
DICE [53]	0.99	0.87	0.82	1.12	0.98	0.95	1.04	0.85
Meta-Self [67]	0.99	0.84	1.16	1.37	0.98	1.46	1.38	1.4
Meta-Train [67]	0.99	0.93	1.17	1.81	0.98	0.73	0.87	1.11
A-Meta-Self [67]	0.99	1.15	1.19	1.59	0.98	1.21	0.99	0.91
A-Meta-Train [67]	0.99	0.94	1.18	1.38	0.98	0.76	0.77	0.69
GraD [30]	0.99	0.97	0.86	1.15	0.98	1.15	1.01	0.96
DGA-FOA (ours)	0.99	0.84	0.82	0.94	0.98	1.06	0.95	0.51
DGA-FDA (ours)	0.99	0.73	1.24	0.94	0.98	1.05	0.88	1.41

**Table 12: Comparison of training time (in seconds), GPU memory occupancy (in MB) after attack between DGA and baselines with 1% perturbation rate. For a fair comparison, all experiments are conducted on a single 24GB NVIDIA RTX A5000 GPU.**

Dataset Method	Citeseer		Cora		PolBlogs	
	Time	Mem.	Time	Mem.	Time	Mem.
Meta-Self [67]	31	7,045	33	7,377	46	5,093
Meta-Train [67]	31	7,045	33	7,377	46	5,093
A-Meta-Self [67]	82	2,641	134	3,769	91	3,289
A-Meta-Train [67]	82	2,641	134	3,769	91	3,289
GraD [30]	32	10,141	35	8,899	43	5,803
DGA-FOA (ours)	14	1,327	15	1,563	13	1,109
DGA-FDA (ours)	17	1,365	24	1,635	8	1,129

**Table 13: Comparison of training time (in seconds), GPU memory occupancy (in MB) after attack between DGA and baselines with 3% perturbation rate. For a fair comparison, all experiments are conducted on a single 24GB NVIDIA RTX A5000 GPU.**

Dataset Method	Citeseer		Cora		PolBlogs	
	Time	Mem.	Time	Mem.	Time	Mem.
Meta-Self [67]	91	12,345	104	14,721	151	11,773
Meta-Train [67]	91	12,345	104	14,721	151	11,773
A-Meta-Self [67]	251	5,621	412	8,667	273	7,749
A-Meta-Train [67]	251	5,621	412	8,667	273	7,749
Grad [30]	96	15,447	106	16,243	138	12,483
DGA-FOA (ours)	14	1,327	15	1,563	13	1,109
DGA-FDA (ours)	17	1,365	24	1,635	8	1,129

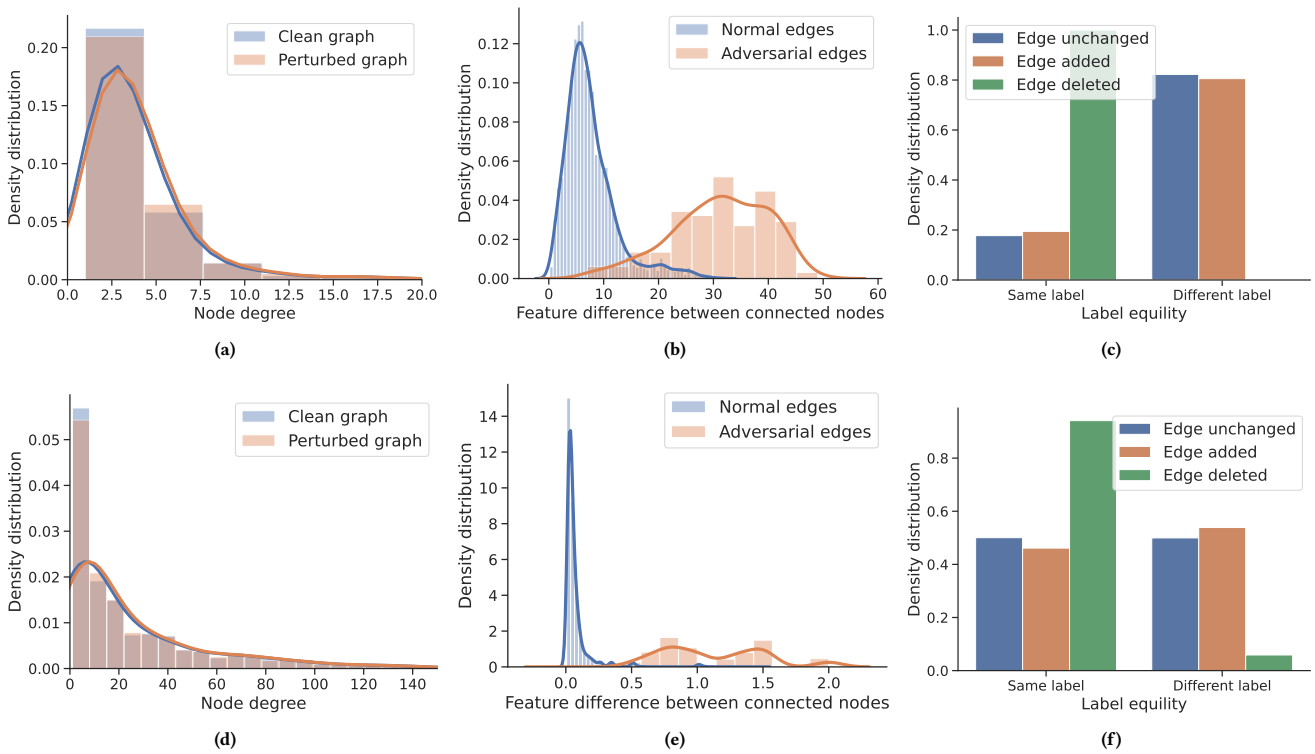


**Figure 4: Visualization of statistics of the poisoned graph compared to the original clean graph on the Cora (upper line) and Polblogs (lower line) datasets. Note that the x-axis of the node degree distribution plot is scaled for better visualization.**